Dynamical Evolution of Planetesimals in the Outer Solar System

II. The Saturn/Uranus and Uranus/Neptune Zones

Kevin R. Grazier

Jet Propulsion Laboratory, California Institute of Technology, Pasadena, California 91109
E-mail: krg@anlashok.jpl.nasa.gov

William I. Newman

Departments of Earth and Space Sciences, Physics and Astronomy, and Mathematics, University of California, Los Angeles, California 90095-1567

Ferenc Varadi

Institute of Geophysics and Planetary Physics, University of California, Los Angeles, California 90095-1567

William M. Kaula

Department of Earth and Space Sciences and Institute of Geophysics and Planetary Physics, University of California, Los Angeles, California 90095-1567

and

James M. Hyman

Theoretical Division, Los Alamos National Laboratory, Los Alamos, New Mexico 87545

We report on numerical simulations exploring the dynamical stability of planetesimals in the gaps between the outer Solar System planets. We search for stable niches in the Saturn/Uranus and Uranus/Neptune zones by employing 10,000 massless particles—many more than previous studies in these two zones—using high-order optimized multistep integration schemes coupled with round-off error minimizing methods. An additional feature of this study, differing from its predecessors, is the fact that our initial distributions contain particles on orbits which are both inclined and non-circular. These initial distributions were also Gaussian distributed such that the Gaussian peaks were at the midpoint between the neighboring perturbers. The simulations showed an initial transient phase where the bulk of the primordial planetesimal swarm was removed from the Solar System within 10^5 years. This is about 10 times longer than we observed in our previous Jupiter/Saturn studies. Next, there was a gravitational relaxation phase where the particles underwent a random walk in momentum space and were exponentially eliminated by random encounters with the planets. Unlike our previous Jupiter/Saturn simulation, the particles did not fully relax into a third Lagrangian niche phase where long-lived particles are at Lagrange points or stable niches. This is either because the Lagrangian niche phase never occurs or because these simulations did not have enough particles for this third phase to manifest. In these simulations, there was a general trend for the particles to migrate outward and eventually to be cleared out by the outermost planet in the zone. We confirmed that particles with higher eccentricities had shorter lifetimes and that the resonances between the jovian planets "pumped up" the eccentricities of the planetesimals with low-inclination orbits more than those with higher inclinations. We estimated the expected lifetime of particles using kinetic theory and even though the time scale of the Uranus/Neptune simulation was 380 times longer than our previous Jupiter/Saturn simulation, the planetesimals in the Uranus/Neptune zone were cleared out more quickly than those in the Saturn/Uranus zone because of the positions of resonances with the jovian planets. These resonances had an even greater effect than random gravitational stirring in the winnowing process and confirm that all the jovian planets are necessary in long simulations. Even though we observed several long-lived zones near 12.5, 14.4, 16, 24.5, and 26 AU, only two particles remained at the end of the 10^9-year integration: one near the $2:3$ Saturn resonance, and the other near the Neptune $1:1$ resonance. This suggests that niches for planetesimal material in the jovian planets are rare and may exist either only in extremely narrow bands or in the neighborhoods of the triangular Lagrange points of the outer planets.   ⓒ **1999 Academic Press**

1. INTRODUCTION

Why is there an apparent lack of planetesimal material between the outer planets in the Solar System? Is it due to observational

bias—the bodies are there, but are distant and dark and just cannot be observed? Did these regions suffer an *ab initio* depletion of planetesimal material for reasons as of yet not understood? Or is it simply that these regions are dynamically unstable over long time periods? This third hypothesis is one we can test. We therefore seek to explore the dynamical stability of planetesimals in the gaps between the outer Solar System planets by simulating the evolution of 10,000 massless test particle placed in each of the interplanet gaps. The particles are initially on random orbits (selected from the prescription described below), and their trajectories are simulated using high-order optimized multistep integration schemes coupled with roundoff error minimizing methods.

In contrast with the Jupiter/Saturn zone, there have been comparatively few computational studies of planetesimal lifetimes in the Saturn/Uranus and Uranus/Neptune zones. This is almost certainly a byproduct of the extreme computational expense that results from the much slower dynamical evolution of these regions when compared to the Jupiter/Saturn zone. Indeed, our present studies—with 10 times fewer particles than our Jupiter/Saturn simulation (Grazier *et al.* 1999, hereafter called Paper I)—took approximately 30 times as many CPU hours. In Paper I we delineated three distinct phases of planetesimal evolution in the Jupiter/Saturn zone. Using kinetic theory to estimate depletion rates for each phase, our *ab initio* calculations predicted that the initial rate of depletion of planetesimals would be a factor of 80 slower in the Saturn/Uranus and Uranus/Neptune zones than in the Jupiter/Saturn zone. Our calculations also indicated that this factor would increase to at least 200 for the second phase. In the simulations, the factor for this second phase of evolution was more nearly 400. In the early stages of this simulation, we employed as many as 50 fast Hewlett–Packard workstations running simultaneously, each having identical planetary positions, but with different planetesimal populations.

There are very few known objects with semimajor axes in the range between Saturn and Neptune. The Jet Propulsion Laboratory maintains the Horizons database of all known Solar System bodies for which the orbits are well-determined (Giorgini *et al.* 1996). This database contains only eight asteroids, known as Centaurs, whose semimajor axes lie in the Saturn/Uranus or Uranus/Neptune zones. Even the term "asteroid" can be nebulous in describing bodies in the outer Solar System because the composition of many such bodies is more cometary in nature. Chiron, probably the most well-known Centaur, has both an asteroid designation (2060 Chiron) and a comet designation (95 P/Chiron). The latter was a result of the observations that Chiron both has a dust coma (Meech and Belton 1989) and exhibits bursts of outgassing (Bus *et al.* 1991). The orbits of all the known Centaur objects are very eccentric and cross the orbits of at least one planet. In fact, 1996 PW is an Earth-crossing asteroid. These planet-crossing asteroids almost certainly have orbits that are unstable over long time periods.

The outer Solar System is also host to a handful of comets whose orbits place them ostensibly in the Saturn/Uranus or Uranus/Neptune zones (by virtue of their semimajor axes, although not necessarily where they spend the majority of their time). Comets whose semimajor axes place them in the Saturn/Uranus zone include Comet P/Halley and the Earth-threatening Comet P/Tempel–Tuttle. In the Uranus/Neptune zone is Comet P/Swift–Tuttle, another Earth-crossing comet, which is associated with the Perseid meteor stream. As with the Centaur asteroids, all of the short-period comets whose semimajor axes lie in the range between Saturn and Neptune are on planet-crossing, hence unstable, orbits.

Our computational simulations support these observations. Like our earlier Jupiter/Saturn study we find that, even taking into account the longer dynamical time-scales associated with these regions, there appear to be no stable niches for planetesimals in the outer Solar System apart, perhaps, from the neighborhood of the triangular Lagrange points of Saturn, Uranus, and Neptune. Though we found one Neptune coorbiter, our initial distributions were biased against finding a large number of outer planet "Trojans."

2. PREVIOUS WORK

There have been several earlier investigations of these regions. In the first of these focused studies, Shoemaker and Wolfe (1984; hereafter SW84) examined the dynamical evolution of planetesimals situated between Uranus and Neptune. Modeling planetary close encounters using Öpik's method, SW84 followed the orbital evolution of 2000 test particles for 4.5 Gyr. They found that the vast majority of the particles initially situated in this zone were ejected from the Solar System. Nine percent of their initial sample survived the entire simulation, however.

In 1989, Duncan *et al.* (1989; hereafter referred to as DQT89) defined a two-adjacent-planet mapping that approximated the restricted three-body problem. In their model, planets were confined to circular, coplanar orbits; test particles had initially small eccentricities and were similarly confined to the invariable plane. Particle orbits were treated as Keplerian, except at conjunctions where they were given impulsive perturbations. Using this mapping method, they examined the zones between each of the outer planets for up to 4.5 Gyr. They found that many of the nearly circular orbits in both the Saturn/Uranus and the Uranus/Neptune gaps might survive over the lifetime of the Solar System—in what they called "Kuiper Bands."

The following year, Gladman and Duncan (1990; hereafter GD90) presented results that were in dramatic contrast with those of DQT89. Using a fourth-order symplectic mapping method developed by Candy and Rozmus (1990), GD90 performed a three-dimensional integration of the trajectories of 180 nearly circular, coplanar zero-inclination particles—90 in each of the Saturn/Uranus and Uranus/Neptune zones—for up to 22.5 Myr. The positions and velocities of the planets in their simulation were not coplanar and were selected according to the LONGSTOP 1B initial conditions (Nobili *et al.* 1989). They found that most of the test particles were removed by close

approaches within 10 Myr. GD90 reported that one band, centered at about 26 AU, contained particles that survived the entire integration while maintaining low eccentricities. They concluded that the survival of this band over Solar System lifetimes was doubtful.

Holman and Wisdom (1993; hereafter HW93) used their symplectic mapping technique (Wisdom and Holman 1991) to survey the outer Solar System for stable orbits in the range from 5 to 50 AU. In the HW93 simulations, the integrations were performed in three dimensions—using three-dimensional initial planetary conditions from Cohen *et al.* (1973)—but with all planetesimals initially on zero-inclination circular orbits. After an 800-Myr simulation, they found that no particles survived between Saturn and Uranus, and only 6 (of 438) survived between Uranus and Neptune. Similar to GD90, 4 of these were near 26 AU. HW93, like GD90, found that most of the test particles in these zones were removed on 10^7-year time-scales. HW93 also performed integrations of particles initially situated at the triangular Lagrange points of the outer three planets. They found that the neighborhood near the L4 and L5 points of Uranus and Neptune was stable for up to 20 Myr. The corresponding points for Saturn were unstable, although particles initially situated in an annular region surrounding the L4 and L5 points were stable for 20-Myr time frames. This last result was corroborated by de la Barre *et al.* (1996), who found Saturn librators (which they termed "Bruins"), which were stable for up to 412 Myr.

Levison and Duncan (1993) and Duncan and Quinn (1993) used a modified Wisdom–Holman scheme, in which the planetary motions were determined from a synthetic secular perturbation theory, and examined these regions for up to 1 Gyr. Using low-inclination, nearly circular orbits, they found that nearly all of the test particles initially in these zones became planet-crossers within 10^8 years—except for a few long-lived bands at 16, 24, and again, 26 AU. All particles became planet-crossing by 10^9 years.

Most recently Holman (1997), also using the Wisdom–Holman symplectic scheme, simulated the orbits of "several thousand" test particles in the Uranus/Neptune zone in the range of 24 to 27 AU. Their orbits were integrated for durations up to 4.5 Gyr. The particles in this simulation had inclined and noncircular orbits, with initial inclinations (i_0) ranging from $0°$ to $10°$, and initial eccentricities (e_0) less than 0.05. Holman found that all test particles with $e_0 > 0.03$ or $i_0 > 3°$ were removed within 1 Gyr, while all test particles with $e_0 > 0.01$ or $i_0 > 1°$ were removed within 4.5 Gyr. The study found that two bands, one near 24.6 AU and the other near 25.6, can preserve planetesimal material for billion-year time periods. In fact, five test particles in the band near 25.6 AU survived the entire 4.5-Gyr simulation, similar to previous studies which suggested a stable band near 26 AU.

3. NUMERICAL METHODS

The numerical method used for the integration is a roundoff-minimized truncation-controlled 13th-order modified Störmer

method. We expanded upon this methodology in Paper I and presented the results of several tests designed to determine the energy and longitude error growth properties of this integration method. A detailed and mathematically rigorous development of this method, as well as related multistep methods, is in Goldstein (1996). Information and test results specific to the integrator used in this study can be found in Grazier (1997). A version of the modified Störmer integrator similar to that used in this study is available on the World Wide Web at `http://pentalith.astrobiology.ucla.edu/varadi/NBI/NBI.html`.

Our simulation began with ten thousand test particles placed in elliptical, inclined heliocentric orbits, and their trajectories were integrated for up to one billion years—a 10-fold increase in time beyond our previously reported results (Grazier *et al.* 1995)—or until they were removed from the simulation. The Sun and all of the jovian planets were included as perturbers and were mutually interacting, but the test particles were treated as massless. Initial planetary positions were determined for one epoch from the DE245 ephemeris (Standish, personal communication, 1994) and were identical to those in our Jupiter/Saturn study. Although input/output was given in heliocentric coordinates, all integrations were performed in a barycentric frame.

The initial test particle semimajor axes were Gaussian-distributed so that the mean semimajor axis peaked at the mean value of the two neighboring planets (14.35 AU for Saturn/Uranus; 24.62 for Uranus/Neptune), and the 3σ points were coincident with the planets' orbits. No orbits were allowed within 0.5 AU of the innermost planet or 0.5 AU beyond the outermost. The initial distributions in inclination, eccentricity, phase angles, longitude of nodes, and longitudes of perihelia were the same as those in our Jupiter/Saturn study.

In this simulation, a test particle was considered to be eliminated if it met one of three criteria—exactly those we used for Jupiter/Saturn. Particles were removed from the simulation if they (1) underwent a close-encounter and passed within the sphere of influence of a planet, (2) were ejected from the Solar System, or (3) collided with the Sun. Further details of the elimination criteria can be found in Paper I. Similar to our Jupiter/Saturn study, no "Sun-grazers" were detected for either Saturn/Uranus or Uranus/Neptune planetesimals.

4. THE SATURN/URANUS ZONE

In Paper I, we delineated three distinct phases in the evolution of particles situated in the interplanet gaps (based upon the number of surviving particles as a function of time): a transient phase, a gravitational relaxation phase, and a Lagrangian/niche phase. Furthermore, we developed a kinetic theory to describe the expected e-folding times for the first two of these phases. Because of the different orbital periods and mass ratios of the neighboring perturbers, we expect to find significant differences in the evolution of the Saturn/Uranus zone—as well as the Uranus/Neptune zone—in comparison with the Jupiter/Saturn zone.
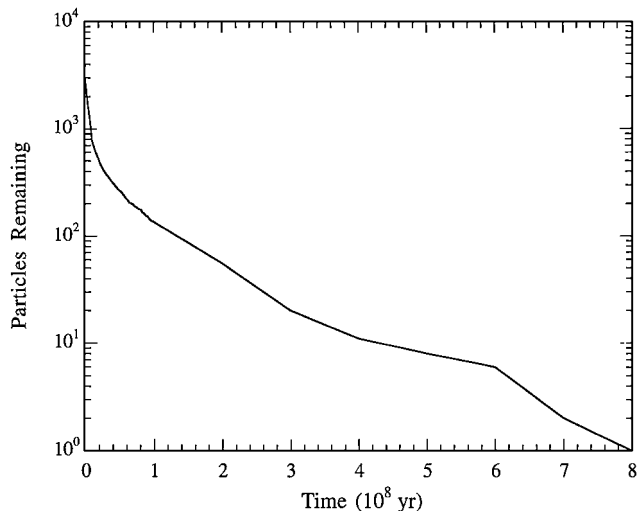
FIG. 1. Number of surviving planetesimals as a function of simulation time for the Saturn/Uranus zone. We see the first two of three phases we delineated in our Jupiter/Saturn study—the system appears to be in transition to the third phase at the simulation's end.

In Fig. 1, we plot the number of surviving planetesimals as a function of time for the Saturn/Uranus zones. The first phase, what we have termed the "transient phase," extends from the beginning of the simulation to 1.0×10^5 years. In this phase, the bulk of the particles removed from the simulation are initially situated in the wings of the distribution and are removed by interacting with the activity spheres (see Paper I) of the neighboring planets by differential rotation. A lesser effect is that many of the very eccentric particles throughout the distribution, regardless of initial semimajor axis, are terminated during this phase.

Based upon this argument, we expect the collision frequency ν to vary as $n\sigma\Delta v$, where n is the number density of colliders (i.e., the jovian planets), σ is the "collision cross section" of the collider, namely πR^2 where R is the radius of the two activity spheres, and Δv is a measure of the velocity difference between planetesimal and planet (Sommerfeld 1956). We used a weighted geometric mean of the activity radii of Saturn (0.36 AU) and Uranus (0.35 AU)—weights appropriate to the ratio of the number of particles removed by Uranus to those removed by Saturn. Taking that ratio to be 1.5 (see Table I), we use $R = R_{\text{Uranus}}^{3/5} \times R_{\text{Saturn}}^{2/5}$, yielding $R = 0.35$ AU.

The number density is estimated from the volume appropriate to our initial planetesimal distribution and has the form of a torus extending between the orbits of the two adjoining planets, subtending an angle normal to the invariable plane with respect to the Sun of $\approx 40°$ (chosen to include 99% of the initial population). We calculated the corresponding volume to be ≈ 9136 AU^3. Because the circular velocity $v \propto a^{-1/2}$, where a is the semimajor axis, we estimated the differential velocity Δv according to the velocity difference between a planet at the center of an activity sphere and a planetesimal on a circular orbit at its periphery, hence $\Delta v \approx (\Delta a/2a)v$, where $\Delta a = R_{\text{act}}$ (where R_{act} is the activity sphere radius). For the Saturn/Uranus

TABLE I

Depletion "Mechanisms" for All Saturn/Uranus Planetesimals as a Function of Their Initial Semimajor Axis Range, in 0.2-AU Increments

| Distance	Alive	Jupiter	Saturn	Uranus	Neptune	Eject
9.0	0	0	3	0	0	0
9.2	0	0	0	0	0	0
9.4	0	0	2	0	0	0
9.6	0	0	8	0	0	0
9.8	0	0	13	0	0	0
10.0	0	0	19	0	0	0
10.2	0	0	21	0	0	0
10.4	0	1	20	5	0	0
10.6	0	0	31	1	1	0
10.8	0	0	44	5	0	0
11.0	0	1	57	5	0	0
11.2	0	1	71	19	2	0
11.4	0	0	71	14	0	0
11.6	0	1	112	20	1	0
11.8	0	0	118	39	0	0
12.0	0	0	137	40	5	0
12.2	0	1	156	46	2	0
12.4	1	4	226	51	4	0
12.6	0	2	233	51	6	1
12.8	0	0	222	75	5	0
13.0	0	3	252	115	1	0
13.2	0	2	250	132	7	0
13.4	0	1	255	164	8	0
13.6	0	0	275	172	12	0
13.8	0	2	283	210	6	0
14.0	0	1	260	242	10	0
14.2	0	1	230	264	8	0
14.4	0	4	222	259	10	0
14.6	0	2	175	285	15	0
14.8	0	0	57	412	0	0
15.0	0	0	30	373	3	0
15.2	0	1	21	377	0	0
15.4	0	0	26	346	4	0
15.6	0	0	22	313	2	0
15.8	0	0	24	291	2	0
16.0	0	0	12	276	2	0
16.2	0	0	9	239	2	0
16.4	0	0	9	205	2	0
16.6	0	0	2	173	0	0
16.8	0	0	6	142	1	0
17.0	0	0	0	112	1	0
17.2	0	0	4	104	1	0
17.4	0	0	4	57	0	0
17.6	0	0	0	64	0	0
17.8	0	0	2	46	0	0
18.0	0	0	2	45	0	0
18.2	0	0	0	14	0	0
18.4	0	0	0	20	0	0
18.6	0	0	0	7	0	0
18.8	0	0	0	6	0	0
19.0	0	0	0	9	0	0
19.2	0	0	0	5	0	0
19.4	0	0	0	1	0	0
Totals	1	28	3996	5851	123	1

zone, we obtained $\Delta v \approx 2.1 \times 10^{-2}$ AU/year. Combining these quantities yields an approximate e-folding time, i.e., the reciprocal of ν, of 5.5×10^5 years while the computational result was 3.5×10^5 years.

In the second, gravitational relaxation, phase, the wings of the particle distribution are replenished as planetesimals undergo a form of random walk in momentum space—caused by intermittent gravitational boosts—as they migrate among the jovian planets. We can employ the Virial Theorem to help us determine the time-scale associated with this process—describing the length of time required for a particle to undergo a major deflection by a planet. We relate Δv to the effective interaction distance r between a planetesimal and a planet of mass M, namely $GM/r \approx \Delta v^2$. Accordingly, we replace the "hard sphere" cross section σ introduced above by the velocity-dependent version $\sigma_{\Delta v}$ according to $\pi r^2 \approx \pi (GM/\Delta v^2)^2$. Then, the appropriate time scale τ varies as $\Delta v^3/\pi n (GM)^2$. This expression shows us that gravitational collision times are smallest when Δv is smallest; hence, planetesimals that closely flank the activity spheres are among the first to be deflected into the path of these spheres of influence. Particles in our simulation initially had a Gaussian distribution with respect to their semimajor axes, and thus those closer to the center of the Gaussian distribution require much more time to complete their random walk into the path of a moving activity sphere. We estimate the lifetime of those particles that must undergo the greatest change in Δv.

We first calculated the velocity of a particle on a circular orbit halfway between Saturn and Uranus, $v_{circ} = 1.66$ AU/year, then approximated Δv by $\Delta v \approx (\Delta a/2a)v$. Our average Δv was 0.56 AU/year. Because we wish to consider gravitational scattering by either Saturn or Uranus, we will employ a weighted geometric mean of their GM values, weighted in the same manner as were the activity radii for the transient phase, giving 3.7×10^{-3} AU^3/year^2. We obtain, therefore, a gravitational relaxation time-scale 1.9×10^7 years, in comparison with our empirical value of 6.4×10^7 years.

We observe here that, by the end of the simulation, the system is making the transition to the third phase, but for the most part this Lagrangian/niche phase is conspicuously absent. We attribute this to two reasons. First, 10^9 years is not sufficient for the full gravitational relaxation of the Saturn/Uranus zone. Second, for our planetesimals, the initial Gaussian distribution in semimajor axis is such that the tails lie at the orbits of Saturn and Uranus. Compared to our Jupiter/Saturn survey, the particle density near the wings is rarefied—we have employed 10 times fewer particles over nearly twice the semimajor axis range. Our initial conditions, therefore, vastly reduce the odds that these simulations will yield Saturn or Uranus coorbiters. Had the system reached full gravitational relaxation (i.e., which perhaps might emerge had the integration been continued to the age of the Solar System), we are not convinced that the third phase would have manifested.

For the first two phases, our kinetic theory yields reasonable order-of-magnitude estimates, but in our Jupiter/Saturn inves-
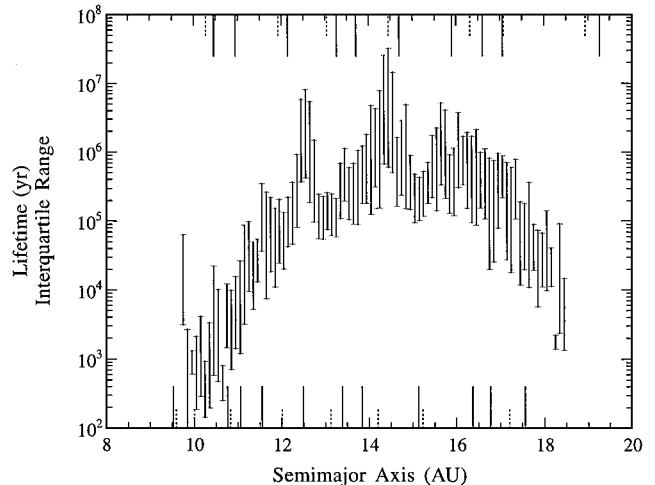
FIG. 2. Particles were grouped according to initial semimajor axes in 0.2-AU intervals and sorted with respect to their lifetimes. High and low values represent the first and third quartiles, respectively. Jupiter and Saturn commensurabilities are indicated across the bottom, while those for Uranus and Neptune are indicated at the top. With the exception of the long-life band centered at 14.2 AU, we see that 75% of the planetesimals are eliminated in 10^7 years. We can also see long-life bands centered at 12.5 and 16 AU.
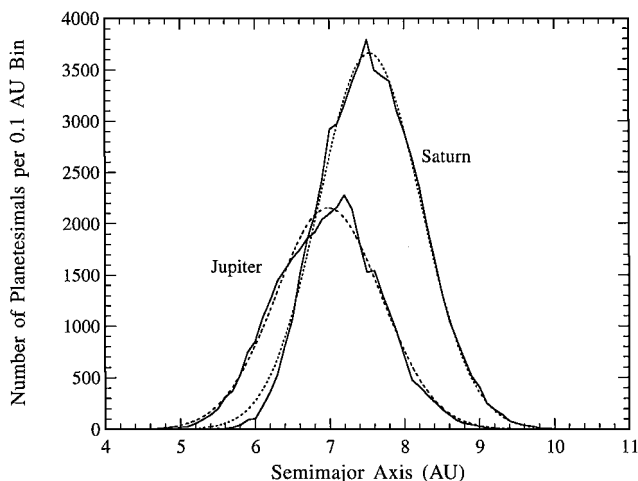
tigation, agreement was substantially better. One possible explanation here is the consequence of our employing a factor of 10 fewer particles. However, we believe that the other planets, particularly Jupiter, have an especially important role in the Saturn/Uranus zone. In addition to Saturn and Uranus, there are a number of resonances from both Jupiter and Neptune which effectively scatter particles throughout the Solar System.

Evidence for this can be seen in Fig. 2. We have grouped the particles by initial semimajor axis in 0.2-AU intervals and sorted the particles in each interval with respect to lifetimes. The high and low values represent the first and third quartiles, respectively. Along the bottom of the figure, we indicate the positions of low-order mean motion commensurabilities of Jupiter and Saturn, while across the top we show commensurabilities with Uranus and Neptune. The location of mean motion commensurabilities that we have indicated are those at the start of the simulation and do not reflect short- and long-term variations of the semimajor axes of any of the planets.
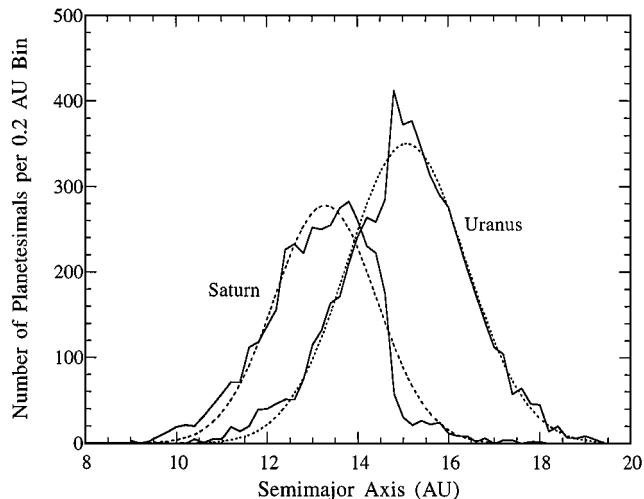
Figure 2 clearly indicates that, with the exception of a band centered at 14.2 AU, the overwhelming majority of the particles in this region are depleted within 10^7 years. In Fig. 2, we also observe rapidly depleted bands whose existence would be difficult to explain merely as the combined effect of Saturn and Uranus. For example, the region from 12.6 to 13.2 AU is a band in which the particle lifetimes are relatively short. The position of this band is not easily explained when we look at Saturn and Uranus alone, but we see that the Jupiter 1:4 mean motion resonance may have aided in clearing this band of planetesimals. If so, this confirms the conclusion in GD90 that, in order to capture the dynamics of the Solar System, any simulation must necessarily include all of the jovian planets.

In Table I we indicate the relative importance of various mechanisms for depleting particles from the Saturn/Uranus zone according to the planetesimals' initial semimajor axes. In each 0.2-AU interval, we enumerate how many test particles survived until the end of the simulation, how many were eliminated through collision with the activity spheres of the jovian planets, and how many were ejected from the Solar System. In our Jupiter/Saturn study, we found that the ratio of particles eliminated by Saturn to that by Jupiter was basically uniform and explicable by simple geometrical–kinetic arguments. Here we see a much more intricate pattern that no longer preserves the ratios and that shows a pronounced asymmetry, which we attribute to the symmetry-breaking influence of Jupiter and, to a lesser extent, Neptune. Also in our Jupiter/Saturn study, we found that a greater number of particles was eliminated by interaction with the activity sphere of the outer planet, rather than by the inner. This is as expected, since a planetesimal on an orbit crossing the orbits of both neighboring perturbers will spend a greater time in the proximity of the outer planet.

In Fig. 3 we plot the number of particles eliminated by Jupiter and by Saturn as a function of initial semimajor axis. This plot yields two Gaussian-like curves, peaked at 6.98 AU (particles eliminated by Jupiter) and 7.54 AU (particles eliminated by Saturn), to which we have fit Gaussian functions in order to determine where the curves are peaked. The peak-to-peak distance is 0.56 AU within an overall range of 4.8 AU. In Fig. 4 we present a similar plot for the Saturn/Uranus zone, indicating the number of particles eliminated through interaction with the neighboring planets. Again, we see two Gaussian-like curves with the outer planet eliminating the majority of the planetesimals. As with Fig. 3, we have plotted the best-fit Gaussian function through the curves to determine where the data are peaked. In Fig. 4 the peaks of the two curves at 13.3 and 15.1 AU have a distance of

FIG. 4. The number of particles eliminated by both Saturn and Uranus as a function of the initial particle semimajor axis. As with Fig. 5, we fit Gaussian functions through the data to indicate more clearly where the results are peaked. We see a much greater splitting of the peaks than in the Jupiter/Saturn zone.

1.8 AU versus a 9.7-AU range. We see two possible reasons for this. Of the zones between the four jovian planets, the mass ratio for the neighboring perturbers is greatest in the Saturn/Uranus zone: 6.5 for Saturn/Uranus, 3.3 for Jupiter/Saturn, and 1.1 for Uranus/Neptune. Additionally, we may also be seeing the combined effects of Jupiter and Neptune.

Complementary to Table I is Table II, in which we present the mean and standard deviation of initial and final semimajor axes for all particles eliminated by the activity spheres of the jovian planets. Further, in Table III, we enumerate the number of particles that ended the simulation with their semimajor axes in various ranges. Three particles ended the simulation having semimajor axes between 5.2 and 9.5 AU—in the Jupiter/Saturn zone. This accounted for less than 3% of our sample. The bulk of the particles, nearly 93%, was situated between 9.5 and 19.2 AU when they were terminated—still in the Saturn/Uranus zone. Despite the general trend of the particles to migrate outward during

FIG. 3. Results taken from our Jupiter/Saturn study indicating the number of particles eliminated by both Jupiter and Saturn as a function of the initial particle semimajor axis. We have fit Gaussian functions through the data to more clearly indicate where each curve is peaked.

TABLE II
Initial and Final Mean Semimajor Axes, and Standard Deviations, of All Saturn/Uranus Planetesimals Eliminated by Each of the Jovian Planets

Planet (AU)	Planetary distance	Planetesimal mean		Planetesimal SD	
		Initial	Final	Initial	Final
Jupiter	5.20	13.24	11.30	1.19	5.28
Saturn	9.54	13.25	13.37	1.21	3.47
Uranus	19.18	15.14	16.08	1.38	1.44
Neptune	30.06	14.00	22.11	1.23	2.61

Note. With the exception of the particles eliminated by the activity sphere of Jupiter, which was only 28 particles, we see an outward migration in the semimajor axes of the planetesimals, even for those eliminated by Saturn.

TABLE III
The Number of Planetesimals Whose Final Semimajor Axes Fell into Various Ranges of Interest

Inner	Number	Outer
$0 \leq a$	3	$a <$ 5.2
$5.2 \leq a$	227	$a <$ 9.5
$9.5 \leq a$	9295	$a <$ 19.2
$19.2 \leq a$	457	$a <$ 30.1
$30.1 \leq a$	12	$a <$ 40.0
$40.0 \leq a$	3	$a <$ 50.0
$50.0 \leq a$	0	$a <$ 60.0
$60.0 \leq a$	0	$a <$ 70.0
$70.0 \leq a$	1	$a <$ 80.0
$80.0 \leq a$	0	$a <$ 90.0
$90.0 \leq a$	1	$a < 100.0$
$100.0 \leq a$	0	$a < 200.0$
$200.0 \leq a$	0	
	1 ejection	

Note. Nearly 93% of the particles initially situated between Saturn and Uranus were still in this zone at the time of their elimination from the simulation. Just under 5% were in the Uranus/Neptune zone; just over 2% were between Jupiter and Saturn. Only three particles were kicked interior to Jupiter, and there was only one ejection.

the simulation, less than 5% ended up in the Uranus/Neptune zone; only 18 planetesimals had semimajor axes beyond that, including one ejection.

This is consistent with the results of our Jupiter/Saturn study and with the results of researchers who have performed computational studies of galaxy dynamics and have seen such a "mass segregation" (Farouki and Salpeter 1982, Farouki *et al.* 1983, Spitzer 1962), where lighter particles migrate outward. Since the planetesimals we modeled were massless, they had no effect upon evolution of the planets. However, we believe that Tables II and III, as well as Fig. 4, indicate that our system at least partially exhibited the mass segregation phenomenon. Particles terminated by collision with the activity sphere of Uranus had semimajor axes that were, on average, nearly 1 AU greater than that with which they began the simulation. Even particles terminated by Saturn had, on average, greater final semimajor axes than initial.

It should be noted that the results of other dynamical simulations of the outer Solar System have indicated that planetesimals situated between the three outer planets may, in fact, have migrated *inward* (Fernandez and Ip 1981, 1983, 1984). These studies, however, included particles of nonnegligible mass and modeled planet/planetesimal close-encounters with an Öpik-type algorithm. This type of algorithm ignores the roles of resonances on dynamical evolution and assumes that all significant orbital changes occur because of planet/planetesimal close-encounters.

In order to visualize the effect of initial inclination on planetesimal lifetimes, we present Fig. 5—remaining planetesimals as a function of time for particles of 0 to 0.5°, $5 \pm 0.5°$, $10 \pm 0.5°$, $15 \pm 0.5°$, and $20 \pm 0.5°$ inclinations. In the Saturn/Uranus zone

we see, as would be expected, that more highly inclined particles generally have increased lifetimes. Any planetary perturbations to low-inclination particles would directly modify the magnitude of the particle's angular momentum. For inclined cases, such perturbations have both an in-plane and an out-of-plane component and affect the orientation of particle's angular momentum vector (i.e., its inclination) in addition to its magnitude. One implication of this is that mean motion resonances with the jovian planets would be much more efficient in "pumping up" the eccentricities of low-inclination planetesimals than those at higher inclinations.

Table IV yields an indication of the relative significance of various mechanisms of depleting the planetesimal swarm as a function of initial planetesimal inclination. In each 1° range, we indicate the number of planetesimals that were eliminated by the activity spheres of the jovian planets, how many were ejected from the Solar System, and how many survived the entire integration. In our Jupiter/Saturn study we sought to explain, through a simple geometric argument, not only why more particles were eliminated through interaction with Saturn's activity sphere as opposed to Jupiter's, but also the ratio. We assumed that the annulus a planet's activity radius sweeps out in an orbit was a target—the ratio of the areas of these annuli should yield a reasonable "back of the envelope" estimate of the ratio of the number of particles eliminated by the activity spheres of the neighboring planets. Using a similar argument, we would expect Uranus to be responsible for eliminating approximately twice the number of particles as does Saturn. In reviewing Table IV, we see that this estimate does not work nearly as well as it did for the Jupiter/Saturn zone and that for particles inclined up to 20°, the actual ratio varies from 1.84 down to 1.12. We can attribute this to two factors. Resonances with all the jovian
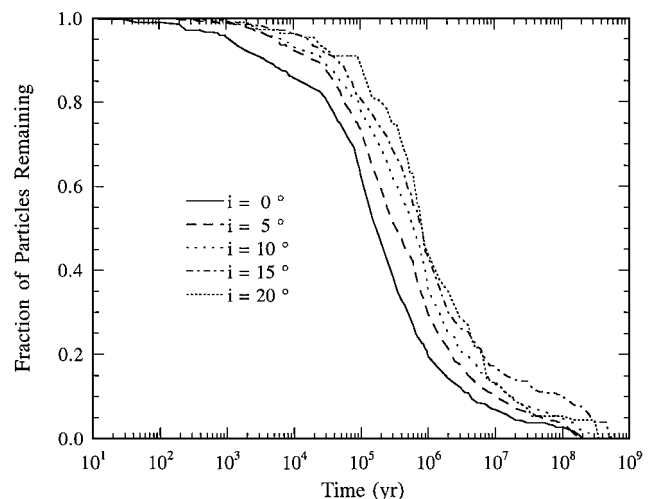
FIG. 5. Fraction of remaining particles as a function of time for inclinations 0, 5, 10, 15, and 20°. Each curve represents particles with initial inclinations $\pm 0.5°$ of the aforementioned values (except for the zero-inclination curve that ranges from 0 to 0.5°. Here we see that the more highly inclined particles generally have longer lifetimes.
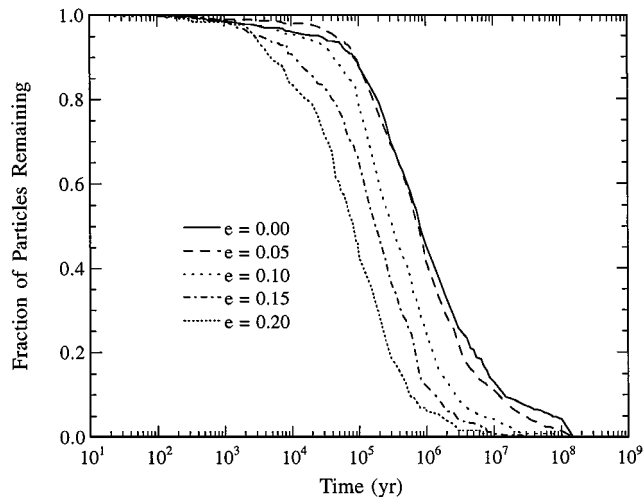
TABLE IV

Depletion "Mechanisms" for All Saturn/Uranus Planetesimals as a Function of Their Initial Inclinations, in 1.0-Degree Increments

Inclination	Alive	Jupiter	Saturn	Uranus	Neptune	Eject
$0 \le i < 1$	1	0	310	500	12	0
$1 \le i < 2$	0	2	258	479	10	0
$2 \le i < 3$	0	1	301	488	12	0
$3 \le i < 4$	0	9	321	444	7	0
$4 \le i < 5$	0	2	256	446	7	0
$5 \le i < 6$	0	2	273	439	11	0
$6 \le i < 7$	0	1	249	378	12	0
$7 \le i < 8$	0	1	254	346	8	0
$8 \le i < 9$	0	2	235	302	8	0
$9 \le i < 10$	0	1	226	292	5	0
$10 \le i < 11$	0	0	186	239	12	0
$11 \le i < 12$	0	1	168	232	2	0
$12 \le i < 13$	0	1	148	179	3	0
$13 \le i < 14$	0	1	130	180	7	0
$14 \le i < 15$	0	3	105	179	2	0
$15 \le i < 16$	0	0	89	139	1	0
$16 \le i < 17$	0	0	88	106	2	0
$17 \le i < 18$	0	0	83	107	1	0
$18 \le i < 19$	0	0	57	65	1	0
$19 \le i < 20$	0	0	54	68	0	0
$20 \le i < 21$	0	0	36	50	0	1
$21 \le i < 22$	0	1	29	45	0	0
$22 \le i < 23$	0	0	28	42	0	0
$23 \le i < 24$	0	0	23	28	0	0
$24 \le i < 25$	0	0	27	16	0	0
$25 \le i < 26$	0	0	15	18	0	0
$26 \le i < 27$	0	0	14	12	0	0
$27 \le i < 28$	0	0	9	6	0	0
$28 \le i < 29$	0	0	7	4	0	0
$29 \le i < 30$	0	0	8	5	0	0
Totals	1	28	3987	5834	123	1

FIG. 6. Similar to Fig. 5, Fig. 6 is a "family of curves" indicating the fraction of particles remaining over time as a function of initial eccentricity. Curves are for eccentricity ranges $0 + 0.025$, 0.05 ± 0.025, 0.10 ± 0.025, 0.15 ± 0.025, and 0.20 ± 0.025. Generally, highly eccentric particles are eliminated quickly, and we are increasingly left with a population of particles that began on more circular orbits. The lone possible exception is for the 0.05 curve that has a depletion rate very similar to that for the 0 eccentricity curve for the first 10^6 years.

for the Saturn/Uranus zone in Fig. 7, in 1-Myr increments ranging from the beginning of the simulation up to 5 Myr. Further, this figure portrays only an approximate representation of the system evolution—we have examined the number of particles surviving at different times in the simulation as a function of their *initial* semimajor axes—the orbits of many particles will have certainly been altered over time. Nevertheless, we clearly see the system quickly evolve into both rapidly depleted and long-life bands. The depleted band at 15 AU corresponds to
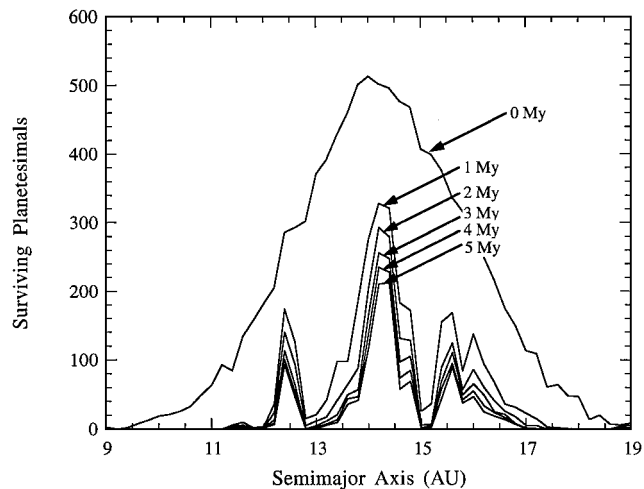
FIG. 7. The number of surviving planetesimals as a function of time and initial semimajor axis range. We see strong resonant effects have quickly depleted bands near 13 and 15 AU, while we see bands at 12.5, 14.4, 15.5, and 16 AU, in which particles are longer lived.

planets have the effect of pumping up the eccentricities for a substantial fraction of the particles so that they cross the orbits of both Saturn and Uranus. This would explain why we see a general outward migration in the semimajor axes of the particles, yet Saturn is responsible for removing a greater-than-expected number of particles. Second, but not as easily quantifiable, we are dealing with a sample size 1/10 that of our Jupiter/Saturn study, and our uncertainties are higher.
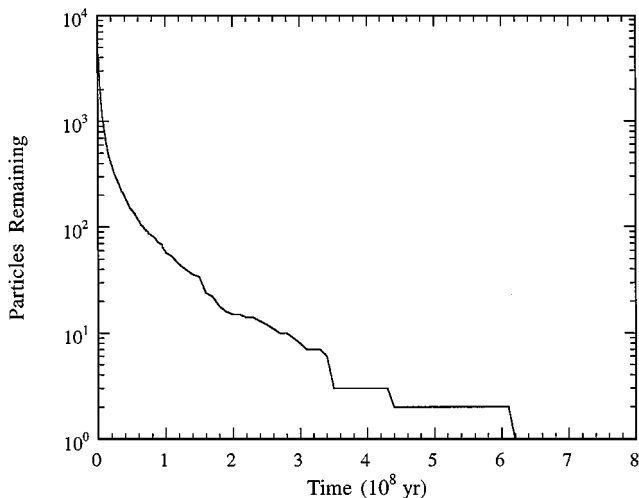
The role of initial eccentricity on particle lifetimes can be see in Fig. 6. Here we examine the number of particles remaining as a function of time for initial eccentricities of $0.00 + 0.025$, 0.05 ± 0.025, 0.10 ± 0.025, 0.15 ± 0.025, and 0.20 ± 0.025. Particles which are more eccentric at the onset of the simulation are, in general, much more short-lived than those on more circular orbits. This is as would be expected and is as we have seen in our previous study.

In Paper I we introduced what we call the "evolution plot" for the Jupiter/Saturn zone, in which we plotted the number of surviving particles as a function of initial semimajor axis at different points in the simulation. We show a similar evolution plot

the Saturn 1:2 mean motion commensurability. However, we observe that Saturn's 2:3 resonance, which is at 12.5 AU, appears stable. We also see a more subtle effect from the Uranus 3:2 and 4:3 commensurabilities at 14.7 and 15.9 AU, respectively. Though this represents only the early evolution of the Saturn/Uranus zone, we can easily identify three, arguably four, long-life bands centered at 12.5, 14.4, 15.5, and 16 AU.

At the end of the simulation, however, only one particle survived the entire 1-Gyr integration. This particle had a semimajor axis of 12.48 AU (just inside the Saturn 2:3 resonance), an eccentricity of 0.055, and an inclination of 1.53°. Though only one particle survived the entire integration, we found three bands of long-lived particles, stable over 100-Myr time periods, centered at 12.5, 14.4, and 16 AU. In a search for stable orbits in the Saturn/Uranus zone over Solar System lifetimes, these bands are the best candidates for a more focused search. Taking into consideration the roles of eccentricity and inclination on planetesimal lifetimes, such a search would be most efficient were it confined to nearly circular orbits over a range of inclinations. Now we turn our attention to the Uranus/Neptune zone, which, as we will shortly see, shows some significant differences as well as some remarkable similarities.

5. THE URANUS/NEPTUNE ZONE

In Fig. 8 we plot the number of surviving planetesimals as a function of time for our Uranus/Neptune zone survey. As with the Saturn/Uranus zone, we find that the system is in transition to the third phase of evolution that we described in our Jupiter/Saturn study—indicating that, like the Saturn/Uranus zone, 10^9 years is not sufficient time for full gravitational relaxation of the Uranus/Neptune zone.

Similar to Saturn/Uranus above, we have estimated the expected lifetimes of particles in the Uranus/Neptune zone using a basic kinetic theory. For the phase that we have termed the "transient" phase, we use a toroidal volume of 30300 AU^3. To estimate the average cross sectional area of the colliders, we used the weighted geometric mean of the activity radii of Uranus ($\approx$0.35 AU) and Neptune ($\approx$0.58 AU) to approximate R, where $R = R_{\mathrm{Neptune}}^{3/5} \times R_{\mathrm{Uranus}}^{2/5}$. R had the value of 0.46 AU, giving a cross section of 0.67 AU^2. To estimate Δv we used the mean difference between the planetary velocities and particles orbiting at their periphery, 1.7×10^{-2} AU/year. Using these values in the equations given above, we find a theoretical time-scale for the transient phase in the Uranus/Neptune zone of 1.34×10^6 years; the computational result was 1.57×10^5 years. Of all our estimates for depletion rates this had, by far, the greatest error.

The gravitational relaxation phase describes the length of time required for a particle to undergo a major deflection by a planet. Again, the first step is to calculate the velocity-dependent collisional cross section. To estimate Δv we first calculated the velocity of a particle on a circular orbit halfway between Uranus and Neptune, $v_{\mathrm{circ}} = 1.27$ AU/year, then approximated Δv by $\Delta v \approx (\Delta a/2a)v$. Our average Δv was 0.28 AU/year. For GM we used the weighted geometric mean of GM_{Uranus} and GM_{Neptune}, 1.9×10^{-3} AU^3/year^2. Hence, for the relaxation phase, our theoretical estimate was 2.9×10^7 year; the simulation value was 5.9×10^7 years. As with Saturn/Uranus, our theoretical estimates for e-folding times for the Uranus/Neptune zone are not as near in agreement with the computational results as were those for Jupiter/Saturn.

It is noteworthy that *all* of the time-scales, for both the Saturn/Uranus and the Uranus/Neptune cases, are much longer than in the corresponding Jupiter/Saturn cases, by as much as a factor of 380. Interestingly, the simulation e-folding times for the Uranus/Neptune zone were actually smaller than those for the Saturn/Uranus zone, suggesting that the Uranus/Neptune zone was, in general, more rapidly evacuated. One potential reason for this is that the ratio of the mean motions of the bounding planets is lower in the Uranus/Neptune zone (2.0) than in the Saturn/Uranus zone (2.8).

In Fig. 9, we examine the expected lifetimes of particles in the Uranus/Neptune zone as a function of their initial semimajor axis (in 0.2-AU intervals). As with Fig. 2, we have indicated the position of several jovian planet mean motion commensurabilities. Jupiter and Saturn resonances are indicated across the bottom of Fig. 9 and those with Uranus and Neptune at the top. In Fig. 9, as with Fig. 2, we see the bulk of the particles are removed from this zone on 10^6- to 10^7-year time-scales.

We note two bands, at 23 and 25 AU, where mean motion commensurabilities appear to have dramatically decreased planetesimal lifetimes. The effect of Jupiter and Saturn on this zone does not appear to be as pronounced as the effect of Jupiter and Neptune on the Saturn/Uranus zone, as could have been expected. The short-life band at 25 AU is coincident with the Neptune 4:3 and Uranus 2:3 commensurabilities. Figure 9 also suggests that there was a long-life band centered at 26 AU, in agreement with results from similar previous studies.

FIG. 8. Number of surviving planetesimals as a function of simulation time for the Uranus/Neptune zone. Here we see a curve very similar to that from our Saturn/Uranus study.

TABLE V

Depletion "Mechanisms" for All Uranus/Neptune Planetesimals as a Function of Their Initial Semimajor Axis Range, in 0.2-AU Increments

Distance	Alive	Jupiter	Saturn	Uranus	Neptune	Eject
18.0	0	0	0	0	0	0
18.2	0	0	0	0	0	0
18.4	0	0	0	0	0	0
18.6	0	0	0	1	0	0
18.8	0	0	0	0	0	0
19.0	0	0	0	2	0	0
19.2	0	0	0	7	0	0
19.4	0	0	0	8	0	0
19.6	0	0	0	23	0	0
19.8	0	0	0	15	0	0
20.0	0	0	0	19	0	0
20.2	0	0	0	30	0	0
20.4	0	0	0	33	0	0
20.6	0	0	0	37	2	0
20.8	0	0	0	54	4	0
21.0	0	0	0	67	4	0
21.2	0	0	1	69	6	0
21.4	0	0	1	81	15	0
21.6	0	0	0	108	22	0
21.8	0	0	0	119	24	0
22.0	0	0	1	134	41	0
22.2	0	0	0	140	38	0
22.4	0	0	0	161	47	0
22.6	0	0	3	174	59	0
22.8	0	0	0	178	67	0
23.0	0	0	2	231	60	0
23.2	0	0	0	225	87	0
23.4	0	0	1	196	157	0
23.6	0	0	0	219	159	0
23.8	0	0	0	196	219	0
24.0	0	0	0	199	202	0
24.2	0	0	1	182	264	0
24.4	0	1	1	175	254	0
24.6	0	0	0	148	290	0
24.8	0	0	0	160	276	0
25.0	0	0	0	140	274	0
25.2	0	0	0	119	266	0
25.4	0	0	1	115	257	0
25.6	0	0	0	90	236	0
25.8	0	0	0	91	243	1
26.0	0	1	0	89	229	0
26.2	0	0	0	74	245	1
26.4	0	0	0	64	203	0
26.6	0	0	2	45	191	0
26.8	0	0	0	38	188	0
27.0	0	0	0	28	179	0
27.2	0	0	0	22	141	0
27.4	0	0	2	18	137	0
27.6	0	0	0	14	112	0
27.8	0	0	0	3	80	0
28.0	0	0	0	9	72	0
28.2	0	0	0	5	47	0
28.4	0	0	0	4	51	0
28.6	0	0	0	4	46	0
28.8	0	0	0	1	29	0
29.0	0	0	0	0	27	0
29.2	0	0	0	0	16	0

TABLE V—*Continued*

Distance	Alive	Jupiter	Saturn	Uranus	Neptune	Eject
29.4	0	0	0	0	21	0
29.6	0	0	0	0	7	0
29.8	1	0	0	0	6	0
30.0	0	0	0	0	6	0
30.2	0	0	0	0	5	0
30.4	0	0	0	0	3	0
30.6	0	0	0	0	1	0
Totals	1	2	16	4364	5615	2

It should be noted that if, over the span of their lifetimes, the planets (particularly Uranus and Neptune) migrated either sunward (Kaula and Newman 1992), or anti-sunward (Fernandez and Ip 1981, 1983, 1984; Malhotra 1993) as a result of interactions with a planetesimal swarm with nonnegligible mass, the positions of mean motion resonances would have "scanned" (cf., Ward 1981), thus sweeping out these regions even more rapidly than indicated in these simulations.

In Table V we examine the termination mechanisms for all particles as a function of their initial semimajor axes in 0.2-AU increments. Consistent with both the Jupiter/Saturn and the Saturn/Uranus zones, we see that collisions with the outer planet's activity sphere, in this case Neptune, are responsible for removing the bulk of the particles. This is consistent with our earlier two simulations in which we saw a general outward migration of the particles, and, in fact, only 18 particles were removed by Jupiter (2) and Saturn (16).

Only two particles were ejected from the Solar System, both of which had inclinations of less than 1 degree. In their simulation
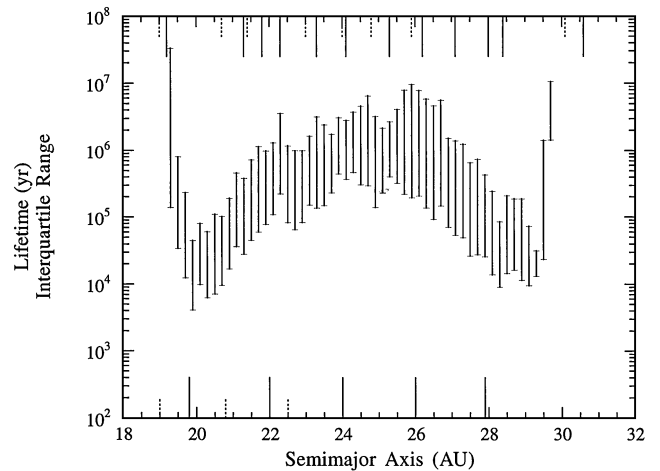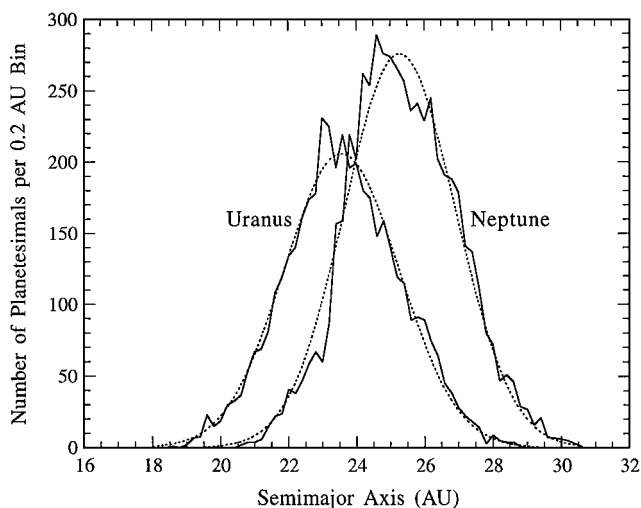

FIG. 9. Similar to Fig. 4, particles were grouped according to initial semimajor axis in 0.2-AU intervals and sorted with respect to their lifetimes. High and low values represent the first and third quartiles, respectively. Jupiter and Saturn commensurabilities are indicated across the bottom, and those for Uranus and Neptune are indicated at the top. We see the long-life band at 26 AU. With the exception of particles near to the Uranus and Neptune 1 : 1 commensurabilities, 75% of the planetesimals are eliminated in 10^7 years.

of the Uranus/Neptune zone, SW84 reported that the "vast majority" of their planetesimals was ejected from the Solar System. The SW84 study used an Öpik algorithm, which, as noted previously, assumes *a priori* that all significant changes in the orbits of the planetesimals arise from close planet/planetesimal encounters. As we have outlined at the beginning, we terminate a particle when it enters the sphere of influence, or activity sphere, of a planet—we make no attempt to model close approaches. On the other hand, Weissman (1994) has argued that neither Uranus nor Neptune are large enough to eject a significant number of comets from the Solar System, so perhaps the high percentage of ejections seen by SW84 was, in fact, an artifact of their numerical methods. Our results not only support this—with only one particle in the Saturn/Uranus zone and two in the Uranus/Neptune zone being ejected—but also suggest that Saturn, too, is not big enough to eject many planetesimals into interstellar space.

In Fig. 10 we plot the number of planetesimals eliminated by the nearest neighbor planets, as a function of initial semimajor axis, and as with Figs. 3 and 4 we have fit Gaussian functions through these curves. We see two peaks, at 23.6 and 25.3 AU, with the outer planet responsible for the elimination of more planetesimals. The peak-to-peak distance in this plot is 1.7 AU over an 11-AU range. Taken together, Figs. 3, 4, and 10 would seem to indicate that Uranus and Neptune had a trivial effect on the dynamics of the Jupiter/Saturn zone, but the combined effect of Jupiter and Neptune on the Saturn/Uranus zone pulled apart the peaks we see in Fig. 4. In the Neptune/Uranus zone, we see the two peaks intermediate in distance between those in the Jupiter/Saturn and Saturn/Uranus zones, suggesting that the combined effect of the inner jovian planet had a lesser, although nontrivial, effect on the dynamics of the Uranus/Neptune zone than in Saturn/Uranus.

TABLE VI
Initial and Final Mean Semimajor Axes, and Standard Deviations, of All Uranus/Neptune Planetesimals Eliminated by Each of the Jovian Planets

Planet	Planetary distance	Planetesimal mean		Planetesimal SD	
(AU)		Initial	Final	Initial	Final
Jupiter	5.20	25.25	24.16	1.20	22.50
Saturn	9.54	24.11	26.00	2.11	6.70
Uranus	19.18	23.70	23.11	1.67	2.14
Neptune	30.06	25.46	26.68	1.60	2.20

Note. The semimajor axes of particles eliminated by the activity spheres of Uranus and Jupiter showed an inward migration, but those eliminated by Neptune and Saturn generally migrated outward. Because Neptune was the planet that eliminated the majority of the planetesimals, we see a general outward migration of planetesimals, consistent with our Jupiter/Saturn and Saturn/Uranus simulations.

Table VI depicts the mean and standard deviation of initial and final semimajor axes for all particles eliminated by the activity spheres of the four planets. Because the particles eliminated by Jupiter and Saturn represent a statistically insignificant subset of the population, we will focus only on those eliminated by Uranus and Neptune. We see that, on average, the particles eliminated by the activity sphere of Uranus migrated approximately 0.6 AU inward, but those eliminated by Neptune migrated 1.2 AU outward. Because Neptune was responsible for eliminating more planetesimals than Uranus, again we see a general outward migration. This effect is corroborated by Table VII, in which we list the number of particles that fell into various semimajor axis

TABLE VII
The Number of Planetesimals Whose Final Semimajor Axes Fell into Various Ranges of Interest

Inner	Number	Outer
$0 \leq a$	0	$a < 5.2$
$5.2 \leq a$	1	$a < 9.5$
$9.5 \leq a$	142	$a < 19.2$
$19.2 \leq a$	9479	$a < 30.1$
$30.1 \leq a$	360	$a < 40.0$
$40.0 \leq a$	4	$a < 50.0$
$50.0 \leq a$	3	$a < 60.0$
$60.0 \leq a$	0	$a < 70.0$
$70.0 \leq a$	0	$a < 80.0$
$80.0 \leq a$	0	$a < 90.0$
$90.0 \leq a$	0	$a < 100.0$
$100.0 \leq a$	0	$a < 200.0$
$200.0 \leq a$	0	
	11 ejections	

FIG. 10. The number of particles eliminated by both Uranus and Neptune as a function of the initial particle semimajor axis. As with Figs. 5 and 6, we fit Gaussian functions through the results to indicate more clearly where they are peaked. We see more splitting of the peaks than in the Jupiter/Saturn zone, but less than Saturn/Uranus.

Note. Nearly 95% of the particles initially situated between Uranus and Neptune were still in this zone at the time of their elimination from the simulation. Only 1.4% were in the Saturn/Uranus zone; just over 3.6% were exterior to Neptune. There were only two ejections.

ranges at the time of their removal from the simulation. Compared to our Jupiter/Saturn and Saturn/Uranus studies, a much greater percentage of particles in the Uranus/Neptune zone finished their lives having semimajor axes in the interplanet zone in which they began the simulation. This is almost certainly due to the comparatively smaller gravitational pull of the neighboring perturbers, along with the much greater distance scales over which these perturbations acted. We see that less than 1.5% of the particles evolved sunward, and approximately 3.6% had semimajor axes greater than that of Neptune. Nearly 95% of the particles were terminated while still, strictly speaking, in the Uranus/Neptune zone.

The particles in this zone were more "confined" than in our Jupiter/Saturn and Saturn/Uranus simulations (i.e., a greater percentage of particles were eliminated while having their semimajor axes still in their original zone). Because a higher percentage of particles in the other two studies migrated outside their initial zones, this functionally increased the volume of their "container," and this would argue that our kinetic theory would have been in *closest* agreement with the actual simulation rates for the Uranus/Neptune zone—instead, agreement with a simple kinetic theory was worse for the zone between the outer two planets.

We suggest that the reason for this is a combination of our choice of initial conditions and the location of a low-order mean motion resonance which manifests in this zone. Our initial particle ensemble was Gaussian-distributed in semimajor axis so that the peak of the distribution was located halfway between neighboring jovian planets. In the Neptune/Uranus case, the peak of this distribution was at 24.6 AU; the Neptune 4 : 3 resonance is at 24.8 AU. Indeed, throughout the Uranus/Neptune zone, low-order commensurabilities are more evenly distributed, rather than "clumped" as in the Saturn/Uranus zone, so we don't see such dramatic peaks in particle lifetimes as we did at 14.4 AU in the Saturn/Uranus zone. The Jupiter/Saturn zone is so dynamically unstable from the gravitational "stirring" of the two largest jovian planets that, even though we clearly saw decreased particle lifetimes at the Jupiter 2 : 3 and Saturn 3 : 5 resonances, it is very likely that resonant effects had a greater relative influence in depleting the Saturn/Uranus and Uranus/Neptune zones. It is likely that this is especially true when the Neptune 4 : 3 resonance manifests itself very near to the peak of the initial distribution.

This effect not only would explain the order-of-magnitude error in our kinetic theory estimate of the Uranus/Neptune transient phase depletion rate, but also would explain why the Neptune/Uranus zone was depleted more rapidly than the Saturn/Uranus gap. In the Saturn/Uranus zone, the peak of the distribution (14.4 AU) was very near the long-life band we reported centered at 14.2 AU. Not only were a large number of Uranus/Neptune zone planetesimals initially situated in a rapidly depleted band, but also a similarly large number of Saturn/Uranus planetesimals were initially located in a long-life band. This would also explain why over twice as many Saturn/Uranus zone planetesimals survived beyond 100 Myr (135) than Uranus/Neptune particles (61). We discuss this further below.
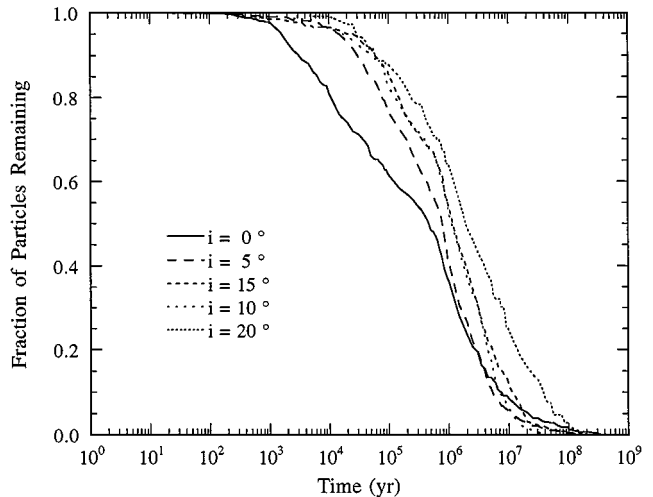
FIG. 11. Fraction of remaining particles as a function of time for inclinations of 0, 5, 10, 15, and 20°. Each curve represents particles with initial inclinations ±0.5° of the aforementioned values (except for the zero-inclination curve which ranges from 0 to 0.5°. The zero-inclination curve has a sharply increased depletion rate for the first 5×10^5 years, with respect particles having more highly inclined orbits. By 3×10^6 years, all surviving particles are either near to the invariable plane or very highly inclined.

As we have done in our previous two studies, we show a "family of curves" in Fig. 11, depicting the comparative depletion rates of particles as a function of their initial inclinations. The tolerance ranges for each curve are the same as for our Saturn/Uranus simulation. Unlike our two previous studies, however, Fig. 11 yields two surprises. The first is that in the first 5×10^5 years of simulation time, planetesimals very near to the invariable plane have a *much* higher depletion rate than those which are inclined even as little as 5°.
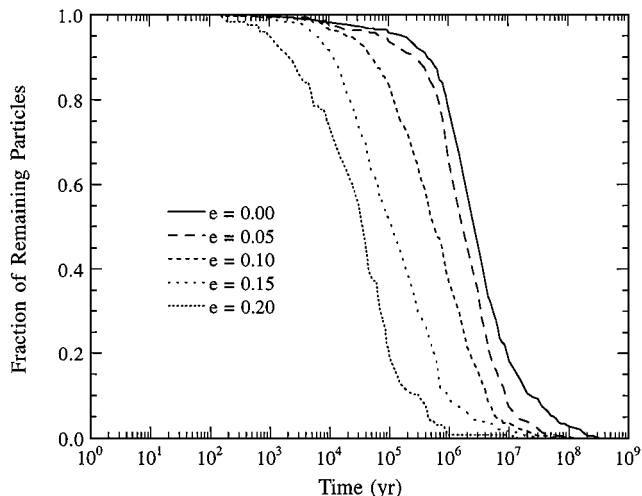
In hindsight, this may not be surprising after all. As we have already pointed out, the eccentricities of low-inclination planetesimals are increased more readily by resonant effects than the eccentricities of more highly inclined bodies. We have also seen that the Neptune 4 : 3 resonance may have been responsible for the elimination of a greater-than-expected number of particles during the transient phase of evolution. It is logical, then, that this and other commensurabilities preferentially affected low-inclination planetesimals, causing an increased depletion of bodies near the invariable plane. The second surprise is that by 5×10^6 years, the zero-inclination curve crosses the 5 and 10° curves. The very long-lived planetesimals, then, are either close to the invariable plane or very highly inclined.

In Table VIII as with Table IV, we enumerate the comparative elimination mechanisms of particles as a function of initial inclination in 1° increments. As with our previous two studies, we see that the outer planet is responsible for eliminating more planetesimals than the inner planet for all inclination ranges, except for the very high inclinations that show the effects of small number statistics.
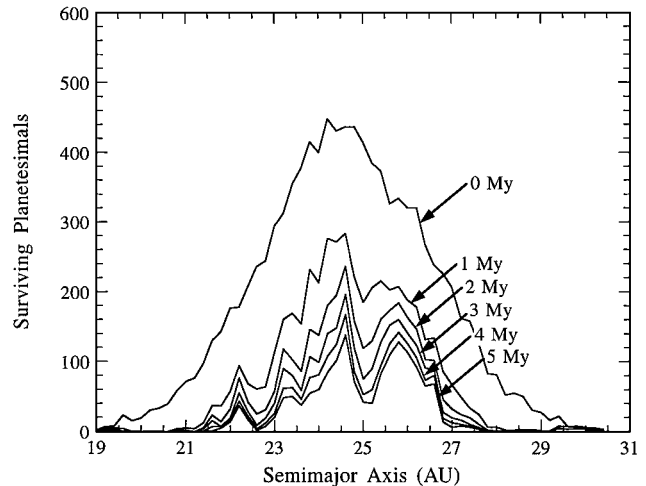
In Fig. 12 we examine the role that initial eccentricity had on particle depletion rates and find no surprises. Figure 12 is

TABLE VIII
Depletion "Mechanisms" for All Uranus/Neptune Planetesimals as a Function of Their Initial Inclinations, in 1.0-Degree Increments

Inclination	Alive	Jupiter	Saturn	Uranus	Neptune	Eject
$0 \le i < 1$	0	0	1	350	471	2
$1 \le i < 2$	0	0	2	308	471	0
$2 \le i < 3$	0	0	0	336	452	0
$3 \le i < 4$	1	0	2	330	457	0
$4 \le i < 5$	0	0	2	282	409	0
$5 \le i < 6$	0	0	1	309	408	0
$6 \le i < 7$	0	0	2	276	354	0
$7 \le i < 8$	0	1	2	282	344	0
$8 \le i < 9$	0	0	0	257	291	0
$9 \le i < 10$	0	0	0	234	277	0
$10 \le i < 11$	0	0	0	199	251	0
$11 \le i < 12$	0	0	0	182	237	0
$12 \le i < 13$	0	0	0	147	163	0
$13 \le i < 14$	0	0	0	153	173	0
$14 \le i < 15$	0	0	2	115	150	0
$15 \le i < 16$	0	0	1	131	121	0
$16 \le i < 17$	0	0	0	74	122	0
$17 \le i < 18$	0	1	0	80	94	0
$18 \le i < 19$	0	0	0	54	72	0
$19 \le i < 20$	0	0	0	53	66	0
$20 \le i < 21$	0	0	0	41	53	0
$21 \le i < 22$	0	0	1	33	37	0
$22 \le i < 23$	0	0	0	31	39	0
$23 \le i < 24$	0	0	0	25	26	0
$24 \le i < 25$	0	0	0	20	24	0
$25 \le i < 26$	0	0	0	15	16	0
$26 \le i < 27$	0	0	0	11	8	0
$27 \le i < 28$	0	0	0	12	6	0
$28 \le i < 29$	0	0	0	6	5	0
$29 \le i < 30$	0	0	0	5	6	0
Totals	1	2	16	4351	5603	2

FIG. 13. The number of surviving planetesimals as a function of time and initial semimajor axis range. We see a more symmetric winnowing and a suggestion that resonant effects are more evenly spaced in the Uranus/Neptune zone than for Saturn/Uranus. We see bands at 22.5, 24.5, and 26 AU in which particles are longer lived.

FIG. 12. "Family of curves" indicating the fraction of particles remaining over time as a function of initial eccentricity. Curves are for the same eccentricity ranges as in Fig. 8. Highly eccentric particles are eliminated quickly, and we are increasingly left with a population characterized by particles that began on more circular orbits.

another family of curves whose parameters are the same as those in Fig. 5. Here we see once again that more eccentric particles are eliminated more quickly.

Figure 13, as with Fig. 7, is an evolution plot of the Uranus/Neptune zone, showing the number of remaining particles as a function of initial semimajor axis at 1-Myr intervals. Qualitatively, we see a much different picture than for the Saturn/Uranus zone. In the Saturn/Uranus zone, we saw how very strong mean motion commensurabilities almost completely deplete bands on very short time-scales, although there are numerous particles in other long-life bands. In the Uranus/Neptune zone, we see neither the very unstable bands nor large numbers of particles in very stable bands. Instead, we see hints of weaker resonances eroding the planetesimal swarm in a more symmetric fashion. As with Fig. 9, we observe a depleted band at 22.6 AU, probably as a result of the Neptune 3 : 2 resonance. We see another centered at 25.2 AU, corresponding to the Uranus 2 : 3 and the Neptune 4 : 3 resonances. We also see hints of long-life bands at 22.4, 23.2, 24.5, and 26 AU.

In similar recent studies, HW93 and Holman (1997) found that particles in the band near 26 AU that are on low-inclination, near-circular orbits can survive for up to 4.5 Gyr. Two factors readily explain the fact that these studies produced survivors in this band, while the present simulation did not. The simulation presented here employed more particles than either of the other two cited works, but the initial distribution included particles over a much wider range of eccentricities. HW93 and Holman (1997) confined their initial trajectories to circular or near-circular orbits. In all three studies, it was the low-eccentricity particles which survive for long time periods. Another factor which could aid in explaining the disparity lies in the fact that the studies used radically different integration techniques. HW93 and Holman (1997) employed the Wisdom–Holman symplectic integration

scheme (Wisdom and Holman 1991), while we have used a more accurate, although computationally slower, modified Störmer multistep integrator.

In the Uranus/Neptune zone, only four particles of the initial 10,000 survived the first 100 Myr, and all were orbits nearly commensurate with Neptune. One of these four particles was the only particle in the simulation to survive the entire 1-Gyr integration time. HW93 showed that particles situated at Neptune's triangular Lagrange points were stable for up to 20 Myr; here we see evidence that they are stable for much longer periods of time.

6. SECULAR INSTABILITIES IN THE SATURN/URANUS AND URANUS/NEPTUNE ZONES

The long-term survival of particles in the outer Solar System is strongly influenced both by mean motion and by secular resonances. The locations of the former are easy to compute. In order to determine the location of secular resonances, however, one has to rely on secular perturbation theory. In this regard, the work most relevant to the present study is that of Knezevic *et al.* (1991). Using a particular averaging method, they determined the location of the most important secular resonances.

Before comparing their predictions with our numerical simulations, we must address three issues. First, the perturbation theory developed by Knezevic *et al.* (1991) is approximate. The underlying problem is sufficiently complex that the details of the calculation should be situation-dependent—i.e., there is no "magic formula." Second, the predictions of Knezevic *et al.* (1991) are expressed in terms of so-called proper elements which emerge from their pertubation theory. Owing to the complexity of their theory, it is very difficult to compute the proper elements, and making detailed comparisons lies beyond the scope of this work. However, the particles which appear to have stable orbits could be excellent test cases for secular pertubation theories. The particle orbits are complicated but sufficiently stable for meaningful estimates of the Fourier spectra of their dynamical variables to be computed. Third, secular resonances, either inside or very close to mean motion resonances, must be treated as special cases (Morbidelli and Moons 1993; de la Barre *et al.* 1996). In general, these are the cases for which theory and simulations disagree most.

In order to estimate the secular frequencies associated with the orbits of stable particles, we computed spectral estimates for many test particles of the variables $e\sin(\varpi)$ and $i\sin(\Omega)$, where e is the eccentricity, i the inclination, ϖ the longitude of perihelion, and Ω the longitude of ascending node. By comparing the spectra of individual particles with those of the major planets, the frequencies of the free oscillations can be determined in many cases. A typical Fourier spectrum for a particle is shown in Fig. 14. Most of the largest peaks, g5 through g8, s6, and s7—using the notation of Knezevic *et al.* (1991)—correspond to perturbations due to the jovian planets (forced oscillations). The peaks g0 and s0 can be identified as the particle's proper or
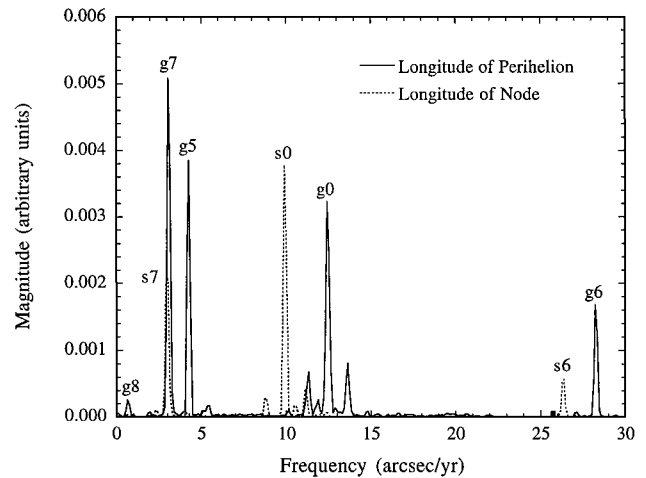

FIG. 14. Fourier spectra of longitudes of perihelion and node for a test particle. The largest peaks can be identifed as perturbations due to the major planets, namely g5 through g8, s6, and s7, using the terminology of Knezevic *et al.* (1991). The peaks g0 and s0 correspond to free oscillations and are flanked by smaller peaks, indicating that the motion is complicated.

free frequencies of perihelion (g0) and node (s0). In a number of cases, the spectra around g0 or s0 have considerable power. These most likely indicate the presence of chaotic components in the orbit. Cases with power in very broad frequency bands were not considered further.

In the Saturn/Uranus zone, there are three clusters of particles with stable orbits for the duration of the simulation. The first one, with semimajor axis near 12.5 AU (Fig. 7), appears to correspond with the 2:3 mean motion resonance with Saturn. The corresponding Fourier spectra are broad in bands at large frequencies and no meaningful estimates of secular frequencies could be obtained.

The particle cluster between 13.6 and 15 AU appears to be far from mean motion resonances. Eccentricities do not exceed 0.1, but inclinations can be as large as 32°. The secular frequencies are easy to determine from Fourier spectra. There are no obvious patterns evident from plots of these frequencies versus semimajor axes or eccentricities. The relationship between frequencies and inclinations in Fig. 15, however, is quite striking. Larger inclinations imply smaller frequencies, since an increase in inclination leads to a decrease in the perturbative torque on orbits. In the case of perihelion frequencies, there appears to be a gap: frequencies near those of the major planets are avoided. Knezevic *et al.* (1991) predict secular resonances between 15 and 20° in inclination. The observed gap in Fig. 15 is at somewhat larger inclinations, as well as broader, but the general agreement—given the imperfectness of the comparison—is good.

The cluster around 16 AU is near the 4:3 mean motion resonance with Uranus. Fourier spectra indicate that regular motion takes place outside of any mean motion resonance. We see this for a particular orbit in Fig. 15. For this orbit, both the eccentricity and the inclination are small, not exceeding 0.066 and 1.8°, respectively. Thus these secular frequencies should be close to
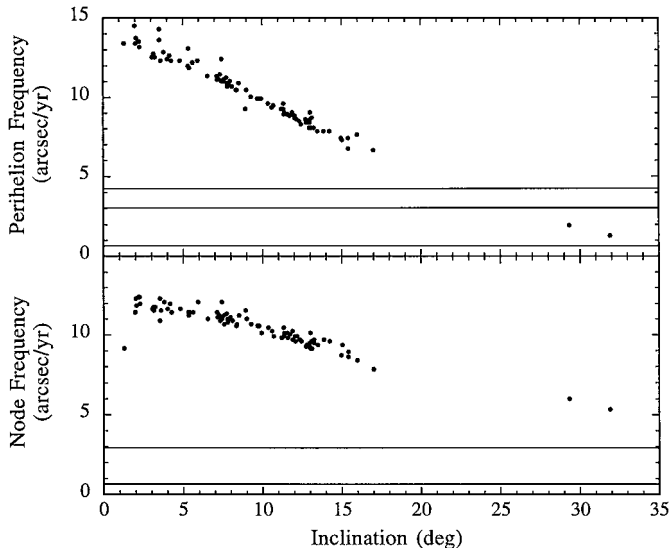
FIG. 15. Secular frequencies of free oscillations in the motion of particles with stable orbits around 14.5 AU. The heavy horizontal lines represent the secular frequencies for the major planets. In the case of perihelia, they are g5, g7, and g8, from top to bottom. There appears to be a wide gap around the g5 and g7 frequencies in the distribution of particles with stable orbits. In the case of nodes, the heavy lines represent s7 (upper) and s8 (lower). The distribution of test particles does not reach low frequency and, thus, the effect of the associated secular resonances cannot be assessed.

those predicted by Knezevic *et al.* (1991). In the case of s0, we have very good agreement (around 10 arcsec/year). In the case of g0, we obtained 12.5 arcsec/year, in contrast with the predicted value of around 30 arcsec/year. The source of this latter discrepancy is not clear.

In the Uranus/Neptune zone, the cluster between 23 and 27 AU shows a gap emerging between 24.8 and 25.2 AU (Fig. 16). The 4 : 3 mean motion resonance with Neptune is at 24.85 AU, which seemingly defines the inner edge of the gap. The frequencies for high inclinations are much smaller than those predicted for low inclinations. For this cluster it is difficult to make meaningful comparisons with predictions, since we are too close to the mean motion resonance. However, overall we find the destabilizing effect of secular resonances is manifest in the absence of stable particle orbits near the secular resonances (denoted by horizontal lines in Fig. 16) of the major planets.

7. CONCLUSIONS

The most important outcome of this study, relevant to our Solar System's origin, is that niches for primordial planetesimal material between the jovian planets will be, if not nonexistent, few and far between. Consistent with other studies, we find long-life bands between the outer planets centered at 12.5, 14.4, 16.0, 24.5, and 26.0 AU. Particles in these bands may be stable on time-scales of up to 10^8 years. Only two planetesimals of 20,000 survived the entire 1-Gyr integration, however: one in each of the Saturn/Uranus and Uranus/Neptune zones. One of

these particles was a Neptune librator, indicating that planetesimals orbiting at the triangular Lagrange point of Neptune may be stable over long time periods.

In comparison with our Jupiter/Saturn study, we see that the time-scales relevant to the dynamical evolution of the outer Solar System are truly different! In the Jupiter/Saturn zone, planetesimals were eliminated on 10^4- to 10^5-year time-scales. Particles in both the Saturn/Uranus and the Uranus/Neptune zones survived much longer, on average, and were eliminated on 10^6- to 10^7-year time-scales.

In our simulations, the Neptune/Uranus zone was depleted more rapidly than the Saturn/Uranus zone, but this was very likely because of the fact that our initial conditions place a large number of Uranus/Neptune zone particles in locations strongly affected by more mean motion resonances. This, perhaps, may also explain why our kinetic theory estimate of planetesimal depletion rates was in much better agreement in both our Jupiter/Saturn and our Saturn/Uranus zone studies. Resonant effects may have also preferentially depleted the Uranus/Neptune zone of low-inclination particles. In comparison to the Jupiter/Saturn zone, resonances appear to have a greater effect in both of these regions than did "gravitational stirring."

The planetesimals in our simulation underwent a general outward migration. This is consistent with the results of our Jupiter/Saturn zone study and with the results of researchers who have performed computational studies of galaxy dynamics and have seen such a "mass segregation" (Farouki and Salpeter 1983; Farouki *et al.* 1983; Spitzer 1962).
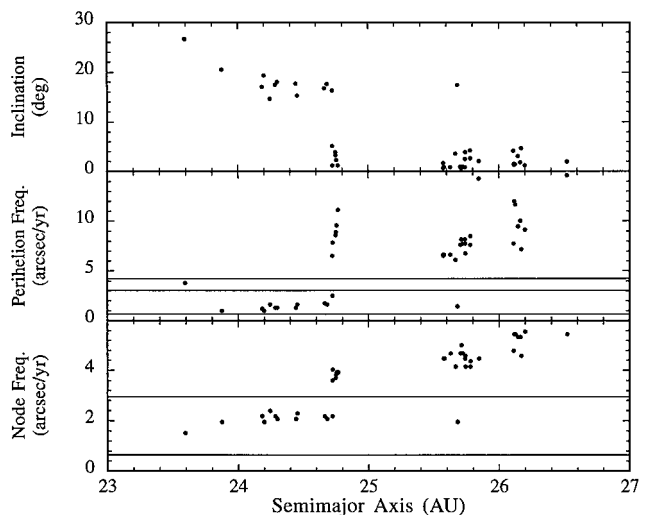
FIG. 16. Mean inclinations (top) and secular frequencies (middle and bottom) in the motion of particles with stable orbits between 23 and 27 AU, as functions of mean semimajor axes. Heavy horizontal lines indicate the secular frequencies of major planets, as in Fig. 15. In the case of perihelia, there is a particle close to g5 but otherwise g5 and g7 appear to define a gap in the distribution. There are several particles, however, near g8. Either the integrations were not long enough or Neptune's eccentricity is too small to cause instabilities in a large part of the phase space. In the case of nodes, s7 seems to correspond to a gap.

REFERENCES

Bus, S. H., M. F. A'Hearn, D. G. Schleicher, and E. Bowell 1991. Detection of CN emission from (2060) Chiron. *Science* **251**, 774–777.

Candy, J., and W. Rozmus 1990. A symplectic integration algorithm for separable Hamiltonian functions. *J. Comput. Phys.* **92**, 230–256.

Cohen, C. J., E. C. Hubbard, and C. Oesterwinter 1973. *Astron. Papers Am. Ephemeris* **22**.

de la Barre, C. M., W. M. Kaula, and F. Varadi 1996. A study of the orbits near Saturn's triangular Lagrangian points. *Icarus* **121**, 88–113.

Duncan, M., and T. Quinn 1993. The long-term dynamical evolution of the Solar System. *Annu. Rev. Astron. Astrophys.* **31**, 265–295.

Duncan, M., T. Quinn, and S. Tremaine 1989. The long-term evolution of orbits in the Solar System: A mapping approach. *Icarus* **82**, 402–418.

Farouki, R. T., and E. E. Salpeter 1983. Mass segregation, relaxation, and the Coulomb logarithm in N-body systems. *Astrophys. J.* **253**, 512–519.

Farouki, R. T., G. L. Hoffman, and E. E. Salpeter 1983. The collapse and violent relaxation of N-body systems: Mass segregation and the secondary maximum. *Astrophys. J.* **271**, 11–21.

Fernandez, J. A., and W.-H. Ip 1981. Dynamical evolution of a cometary swarm in the outer planetary region. *Icarus* **47**, 470–479.

Fernandez, J. A., and W.-H. Ip 1983. On the time evolution of the cometary influx in the region of the terrestrial planets. *Icarus* **54**, 377–387.

Fernandez, J. A., and W.-H. Ip 1984. Some dynamical aspects of the accretion of Uranus and Neptune: The exchange of orbital angular momentum with planetesimals. *Icarus* **58**, 109–120.

Giorgini, J. D., D. K Yeomans, A. B. Chamberlin, P. W. Chodas, R. A. Jacobsen, M. S. Keesey, J. H. Lieske, S. J. Ostro, E. M. Standish, and R. N. Wimberly, 1996. Horizons: JPL's on-line Solar System data service. *Bull. Am. Astron. Soc.* **29**, 1099.

Gladman, B., and M. Duncan 1990. On the fates of minor bodies in the outer Solar System. *Astron. J.* **100**, 1680–1693.

Goldstein, D. 1996. *The Near-Optimality of Störmer Methods for Long Time Integrations of $y'' = g(y)$*. Ph.D. Dissertation, Department of Mathematics, University of California, Los Angeles.

Grazier, K. R. 1997. Ph.D. Dissertation, *The Stability of Planetesimal Niches in the Outer Solar System: A Numerical Investigation*. Department of Earth and Space Sciences, University of California, Los Angeles.

Grazier, K. R., W. I. Newman, W. M. Kaula, and J. M. Hyman 1999. Dynamical evolution of planetesimals in the outer Solar System. I. The Jupiter/Saturn zone. *Icarus* **140**, 340–351.

Grazier, K. R., W. I. Newman, W. M. Kaula, F. Varadi, and J. M. Hyman 1995. An exhaustive search for stable orbits in the outer solar system. *Bull. Am. Astron. Soc.* **27**, 1204.

Holman, M. J. 1997. A possible long-lived belt of objects between Uranus and Neptune. *Nature* **387**, 785–787.

Holman, M. J., and J. Wisdom 1993. Dynamical stability in the outer solar system and the delivery of short period comets. *Astron. J.* **105**(5), 1987–1999.

Kaula, W. M., and W. I. Newman 1992. The origin of Neptune. *Adv. Space Res.* **12**, 3–10.

Knezevic, Z., A. Milani, P. Farinella, Ch. Froeschle, and Cl. Froeschle 1991. Secular resonances from 2 to 50 AU. *Icarus* **93**, 316–330.

Levison, H. F., and M. J. Duncan 1993. The gravitational sculpting of the Kuiper belt. *Astrophys. J.* **406**, L35–L38.

Malhotra, R. 1993. The origin of Pluto's peculiar orbit. *Nature* **365**, 819–821.

Meech, K. J., and M. J. S. Belton 1989. *IAU Circ.* **4770**, April 11.

Morbidelli, A., and M. Moons 1993. Secular resonances inside mean motion commnesurabilities: The 2/1 and 3/1 cases. *Icarus* **102**, 316–332.

Nobili, A. M., A. Milani, and M. Carpino 1989. Fundamental frequencies and small divisors in the orbits of the outer planets. *Astron. Astrophys.* **210**, 313–336.

Öpik, E. J. 1976. *Interplanetary Encounters*. Elsevier, New York.

Shoemaker, E. M., and R. F. Wolfe 1984. Evolution of the Uranus–Neptune planetesimal swarm. *Lunar Planet Sci. Conf.* **15**, 780–781.

Sommerfeld, A. 1956. *Thermodynamics and Statistical Mechanics* (F. Bopp and J. Meixner, Eds.). Translated by J. Kestin. Academic Press, New York.

Spitzer, L., Jr. 1962. *Physics of Fully Ionized Gases*, Second Revised ed. Interscience, New York.

Ward, W. R. 1981. Solar nebula dispersal and the stability of the planetary system. *Icarus* **47**, 234–264.

Weibel, W. M., W. M. Kaula, and W. I. Newman 1990. A computer search for stable orbits between Jupiter and Saturn. *Icarus* **83**, 382–390.

Weissman, P. R. 1994. Why are there no interstellar comets? *Bull. Am. Astron. Soc.* **20**, 1021.

Wisdom, J., and M. Holman 1991. Symplectic maps for the N-body problem. *Astron. J.* **102**, 1528–1538.